Research paper

Preparation of MCM-41 Supported Benzene Sulphonic Acid, a Catalyst for the Synthesis of CL-20 from TAIW

Shixiong Chen,[1*] **Chaofei Yang**,[1] **Hua Qian**,[1**] **Dabin Liu**,[1] **Wang Kai**,[1] **Rui Li**[2]

[1] *School of Chemical Engineering, Nanjing University of Science and Technology, 200 Xiaoling Rd, Nanjing, 210094, China*

[2] *ZNDY Ministerial Key Laboratory, Nanjing University of Science and Technology, 200 Xiaoling* Rd, *Nanjing, 210094, China*
E-mails: *shixiong_chen@126.com; **iem_liu@163.com

Abstract: Pure MCM-41 anchored benzene sulphonic acid (BSA/MCM-41), an efficient heterogeneous catalyst, was prepared for the synthesis of CL-20 from TAIW. The prepared catalysts were fully characterized by FTIR, XRD, TEM, TG, N_2 adsorption techniques, elemental analysis and acidity tests. It was observed that the catalyst (BSA/MCM-41) retained the mesoporous structure like MCM-41, exhibited excellent thermal stability and high activity. Compared with a blank, the high catalytic activity promoted shorter reaction times by a factor of 3/5. In addition, this catalyst could be reused at least five times without significant loss of its catalytic potential. Moreover, the BSA/MCM-41 catalyst exhibited an optimal catalytic performance, with a high to excellent yield of CL-20 (92.5%) with a purity of 98.3%, under the optimum synthesis conditions.

**Keywords:** CL-20, catalytic, MCM-41, benzene sulphonic acid, TAIW

1   Introduction

2,4,6,8,10,12-Hexanitro-2,4,6,8,10,12-hexaazaisowurtzitane (CL-20) is a nitramine with a cage structure. Its successful synthesis has been praised as a breakthrough in the history of explosive synthesis [1]. As one of the most powerful and promising high explosives, CL-20 has been applied in all classes of explosive compounds including cast cure, melt cast, and pressed explosives [2, 3]. The preparation of CL-20 is a multi-step process and several substituted 2,4,6,8,10,12-hexaazaisowurtzitane compounds are used as CL-20 precursors [4]. The last step in the preparation of CL-20 involves the nitrolysis of one of these precursors. In this regard, several nitrolysis systems have been applied, such as nitrating acid and 1-methylimidazolium hydrogensulfate ([Hmim][HSO$_4$])/HNO$_3$ [5, 6]. Hitherto, a mixture of concentrated nitric acid and sulphuric acid in different proportions is the classical nitrolysis method. However, the large amount of sulphuric is difficult to dispose of and often leads to a serious pollution threat to the environment [3]. This obvious drawback has prompted a search for more environmentally-friendly methods that do not require such strong mixed acids and N$_2$O$_4$. Fortunately, many nitration methods avoiding the use of acidic mixtures have been published [7-9]. N$_2$O$_5$/HNO$_3$ as a greener system was used by Qian *et al.* [10-12] for the nitrolysis of tetraacetylhexaazaisowurtzitane (TAIW) to CL-20. Since TAIW has a highly strained cage structure with four groups available to be nitrolysed, it is difficult to completely nitrate TAIW by N$_2$O$_5$/HNO$_3$ without a catalyst, and only 82.3% yield of CL-20 could be achieved. Although the yield of CL-20 could be increased to 89.5% and 94.5% in the presence of surfactants and ionic liquid catalysts, respectively, such catalysts were difficult to recycle and reuse in the homogeneous reaction [13, 14]. Meanwhile, solid acid catalysts have attracted much attention in organic synthesis due to the easy work-up procedures, easy filtration, and minimization of cost and waste generation due to reuse and recycling of the catalysts [15-17]. They have many advantages over liquid acid catalysts, such as being environmentally benign and presenting fewer disposal problems.

Therefore, this study was performed in order to avoid using such mixed acids in the final step of the CL-20 synthesis. Pure MCM-41 mesoporous molecular sieves grafted with benzene sulphonic acid (BSA) were prepared and characterized by FTIR, XRD, nitrogen physisorption, TEM and TG tests. The prepared BSA/MCM-41 was used as a greener system for the synthesis of CL-20 from TAIW for the first time. Additionally, the reaction parameters have been optimized and the product obtained was characterized using HPLC and NMR techniques.

2   Experimental Section

2.1 Chemicals

All of the chemicals used were of AR grade. Phenyltriethoxysilane, toluene, chlorosulfonic acid, chloroform, fuming nitric acid, and TAIW were purchased from Sinopharm Chemical Reagent Company Limited. Siliceous MCM-41 ($S_{BET} = 1074.65$ m^2/g) was purchased from the catalyst factory of Nankai University.

2.2 BSA/MCM-41 catalyst preparation and procedure

The synthetic procedure for BSA/MCM-41 is illustrated in Scheme 1. MCM-41 (5.0 g), after vacuum drying at 393.15 K for 8 h, was placed in a 250 mL two-necked flask, and then a solution of phenyltriethoxysilane (3.0 g) in dry toluene (125 mL) was added. The mixture was refluxed for 24 h under a nitrogen atmosphere, and the resultant solid was filtered off and washed thoroughly with toluene to obtain B/MCM-41. The B/MCM-41 was then impregnated with a chloroform (125 mL) solution of chlorosulfonic acid (5 mL). After being impregnated at 343.15 K for 6 h, the admixture obtained was filtered and rinsed with chloroform. Finally, the BSA/MCM-41 was obtained by roasting the solid at 353.15 K for 5 h.

Scheme 1. Synthetic procedure for BSA/MCM-41

2.3 Preparation of the HNO$_3$ electrolyte

The HNO$_3$ electrolyte was prepared by controlled potential oxidation (approximately +1.85 V) of dinitrogen tetroxide in anhydrous nitric acid at platinum-supported iron oxide anodes [18-20]. The content of N$_2$O$_5$, N$_2$O$_4$, and HNO$_3$ varied with time and can be analyzed according to Chapman and Smith [21]. The final composition of the electrolyte obtained was 15 wt.% N$_2$O$_5$, 3 wt.% N$_2$O$_4$, and 82 wt.% HNO$_3$.

2.4 General procedure for the nitrolysis of TAIW to CL-20

The synthetic procedure for the nitrolysis of TAIW to CL-20 is illustrated in Scheme 2 and the preparation was as follows:

(1) HNO_3 electrolyte (40.0 g) (15 wt.% N_2O_5, 3 wt.% N_2O_4, and 82 wt.% HNO_3) was placed in a flask immersed in an ice water bath;

(2) TAIW (4.5 g) was added in portions, and the mixture was stirred until the substrate was adequately dissolved;

(3) pretreated BSA/MCM-41 was added in solvent, and then the mixture was heated to the optimum reaction temperature;

(4) after complete reaction, distilled water (40 mL) was added dropwise to the reaction solution and stirred for 1 h, the deposited solid was filtered off, washed with water, and dried in a vacuum.
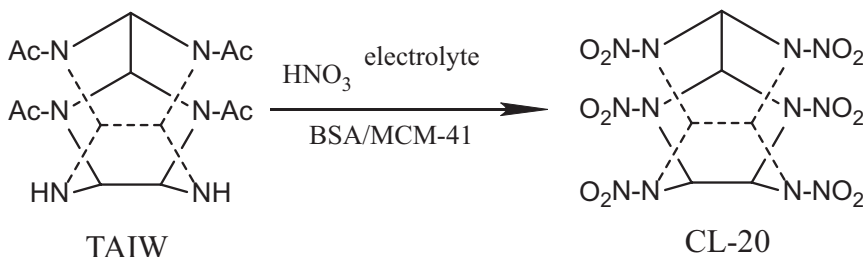
Scheme 2. Synthesis of CL-20

2.5 Experimental techniques

The infrared spectra were recorded on a Shimadzu FT-IR 8400 spectrophotometer. The XRD study of the ordered mesoporous silicas functionalized with the anchored benzene sulphonic group was performed on a Bruker D8 X-ray powder diffractometer (Bruker, Germany), using Cu-Kα radiation ($\lambda = 0.154$ nm) at a scanning rate of 2°/min with a 2θ angle range of 1° to 10°. The specific surface area and pore size distribution of the solids were measured by recording the nitrogen adsorption/desorption isotherms at liquid nitrogen temperature (77 K), using a Micromeritics ASAP-2010 system. Transmission electron micrographs (TEM) were recorded on a JEOL 200CX microscope operating at 200 kV. TG analysis was carried out on a NETZSCH TG 209 F3 instrument with a temperature range of 50-1000 °C, heating rate of 10 K/min and nitrogen atmosphere. The CL-20 was analyzed by high performance liquid chromatography (HPLC) using a C18 column and a methyl alcohol/water mixture as eluent, volume ratio of 50:50, flow rate 1 mL/min. The analysis was carried out at 313.15 K, using a UV detector at 230 nm wavelength.

3　Results and Discussion

3.1　Characterization

The structures of MCM-41 and BSA/MCM-41 were determined by comparing the characterizations by FTIR, XRD, TEM and nitrogen physisorption, and considering whether grafting benzene sulphonic acid onto the MCM-41 had a great impact on the uniform mesoporous structure of MCM-41. Furthermore, TG analysis was used to evaluate the stability of the grafted organic layer.

3.1.1 FTIR spectroscopy

Figure 1 shows the FTIR spectra of MCM-41 and the successful loading of BSA onto MCM-41, in the 400-4000 cm^{-1} range. Clearly, similar peak positions are observed in all of the samples studied. The broad absorption bands at 3440 cm^{-1} are attributed to the hydroxyl groups [22-24] and the band at *ca.* 1638 cm^{-1} is assigned to the bonding vibration mode of the interlayer water molecules. The peak at 1395 cm^{-1} is related to the overtone of the O–H stretching mode [25-27]. A large band in the range of 809-1235 cm^{-1}, assigned to the typical features of silica based materials, contains the Si–O–Si asymmetric stretching and Si–OH stretching of terminal silanols. In the case of BSA/MCM-41 samples, the characteristic peaks of v(S=O) stretching vibrations were located at 1181 cm^{-1}, which could be attributed to the undissociated –SO$_3$H groups [28, 29]. In addition, the peaks observed at 1619 and 1452 cm^{-1} could be assigned to the vibrations of the benzene ring skeleton, which is consistent with previous literature reports [28, 29].
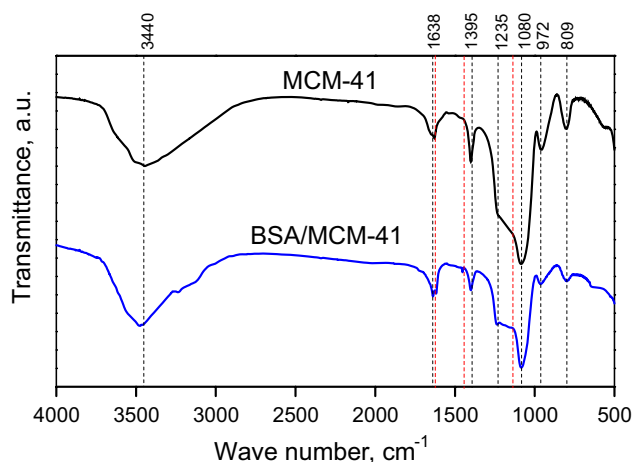

Figure 1.　FTIR spectra of MCM-41and BSA/MCM-41

3.1.2 XRD analysis

Figure 2 shows the small-angle XRD patterns of purely siliceous MCM-41 and BSA/MCM-41. A typical XRD pattern, consisting of one large peak along with two small peaks, which is characteristic of MCM-41, was also observed for BSA/MCM-41. The similar XRD patterns between the prepared BSA/MCM-41 and MCM-41 indicated that the anchoring process did not cause a significant effect on the mesoporous silica material. Compared with the XRD pattern of pure silicon MCM-41, the intensities of the crystal planes (110) and (200) were almost unchanged, which indicated that the long-range ordering of the mesoporous silica material was not affected by the anchoring of the benzene sulphonic acid groups. It is worth noting that the intensity of the crystal plane (100) was dramatically decreased. This may be related to individual differences in the MCM samples, preparation conditions and damaged crystal structure of the mesoporous silicas, partly as a result of the presence of a high population of strong Brønsted acid sites formed during the covalent anchoring [30].
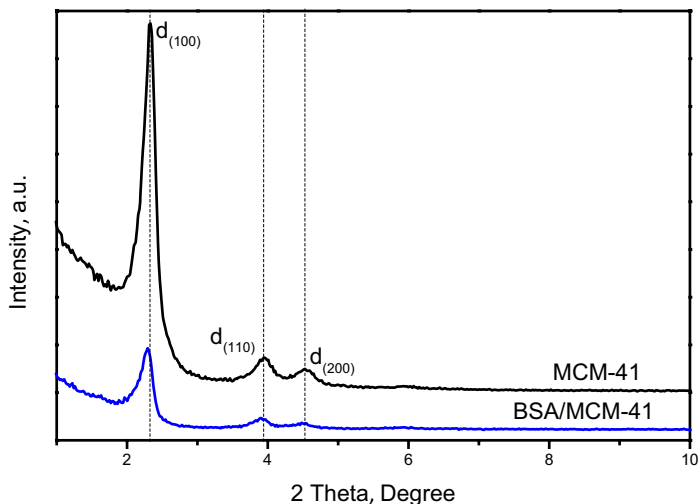

Figure 2.   XRD plot of MCM-41 and BSA/MCM-41

3.1.3 N₂ sorption analysis

Nitrogen adsorption and desorption isotherms of the BSA/MCM-41 samples were measured to further evaluate their surface and textural properties. Figure 3 shows the nitrogen sorption isotherms of MCM-41 and BSA/MCM-41 samples. Both samples exhibit isotherms of type IV with hysteresis loops, which are characteristic of uniform mesoporous materials. The adsorption and desorption isotherms show a large increase in the relative pressure (P/P_0) range from 0.28

to 0.45 for the BSA/MCM-41 samples, due to the capillary condensation of nitrogen within the mesopores [31]. The sharpness of the inflection step reflects the uniform pore size distribution, and the P/P_0 position is clearly related to the diameter in the mesopore range. The second step in the isotherms at $P/P_0 > 0.9$, which was observed for all samples, and is attributed to the condensation of nitrogen in the depressions of a rough surface or between small particles [32].

Pore distribution for all of the supports is mono-modal, further proving that they are mesoporous materials. Figure 4 shows the distributions of BJH desorption average pore diameter. It can be observed that the main peak intensity of BSA/MCM-41 is lower and the pore diameter is smaller than that of MCM-41. It derives from size reduction of larger pores (see TEM characterization below) as a result of the reaction with modifying agents.

The surface area and pore parameters of both samples are listed in Table 1. The surface areas were measured by the BET method, and the pore volumes were calculated from the desorption branch by the BJH method. After addition of the BSA groups on the support, the surface area and pore volume of the catalysts decreased to some extent. The decrease of the BET surface area was attributed to the incorporation of the BSA groups. A certain proportion of BSA groups introduced into the pores occupied this space. In spite of the large amount of BSA groups that had been introduced, a relatively high BET surface area was still maintained, 1074.65 m^2/g for MCM-41 and 813.48 m^2/g for the BSA/MCM-41 sample. Decreases in pore volume and size were also observed, which agrees with the loss of surface area.
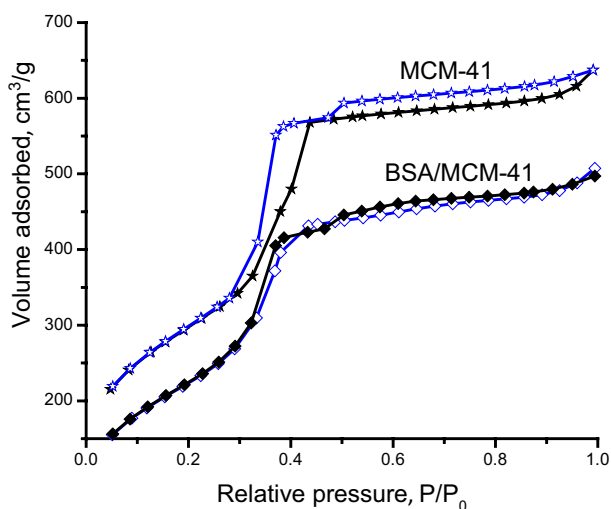

Figure 3.   N$_2$ absorption-desorption curves of MCM-41 and BSA/MCM-41 catalysts
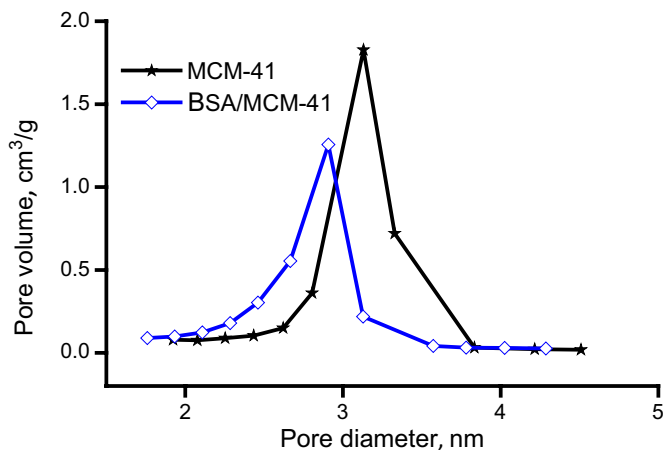
Figure 4.   Pore size distributions of MCM-41 and BSA/MCM-41 catalysts

**Table 1.**   Textural properties of the MCM-41 and BSA/MCM-41 samples

| Sample	S_{BET} [m²/g]	Pore size[a] [nm]	V_{BJH} [cm³/g]
MCM-41	1074.65	3.27	1.07
BSA/MCM-41	813.48	3.02	0.81

[a] Average pore diameter by BJH

3.1.4 TEM images

The XRD and N_2 sorption results were further confirmed by TEM analysis. Figure 5 shows some representative TEM micrographs of MCM-41 and BSA/MCM-41. As can be seen in Figure 5a, the surfactant templated channels, typical of mesoporous silica, are clearly visible in MCM-41. A closer look at the microstructure of the starting MCM-41 clearly shows the hexagonal symmetry of the mesostructure and the section of larger mesopores can be also observed. The porous structure observed by the TEM investigation is in agreement with the N_2 sorption data (Figure 3), which points to the occurrence of secondary mesoporosity responsible for the capillary condensation at high relative pressure in addition to the ordered mesostructure. Figure 5b shows representative TEM images of the hybrid MCM-41 obtained by functionalization with benzene sulphonic acid. It can be clearly inferred that the hybrid materials retain the porous structure of the original MCM-41 silica. However, a mass of benzene sulphonic acid was adsorbed onto the surface of the MCM-41 during functionalization, and which occupied the pore channels so that the channels in BSA/MCM-41 are partially collapsed, to some degree, into disordered and wormhole-like packings. In fact, both the ordered mesoporosity

and the secondary larger mesopores that are observed in the MCM-41 silica, are also present in the hybrid materials, and conforms with the XRD data.
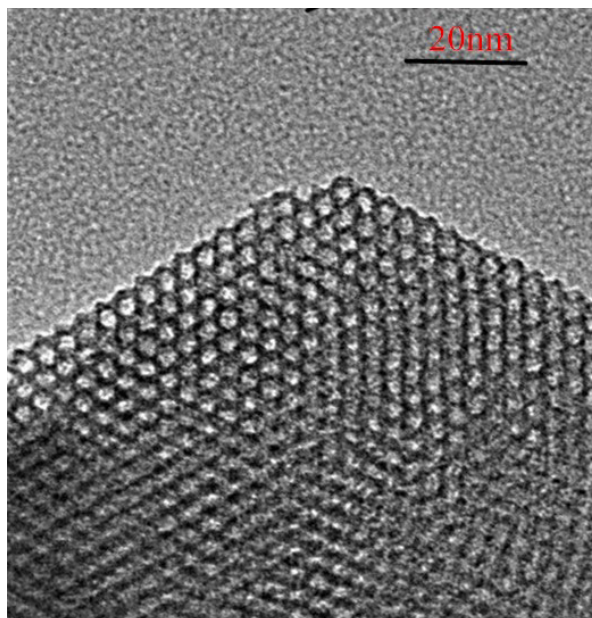
(a)
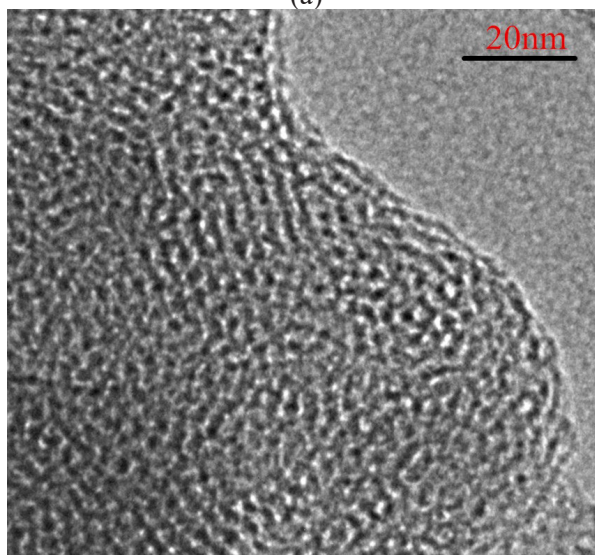
(b)

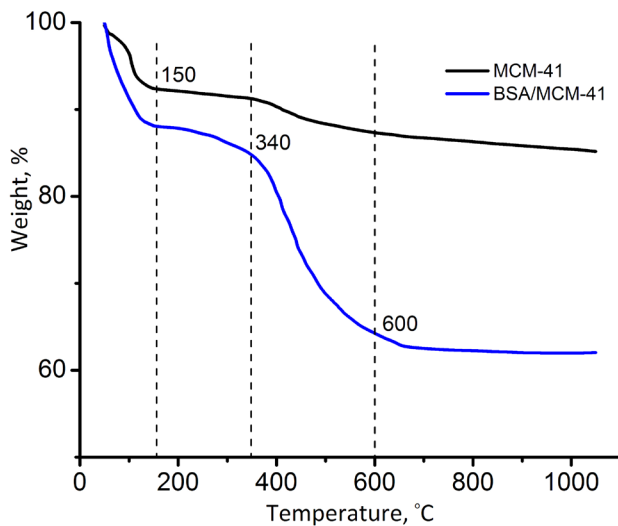**Figure 5.**   TEM images of MCM-41 (a) and BSA/MCM-41 (b)

Figure 6.   TG curves of MCM-41 and BSA/MCM-41

3.1.5 TG analysis

The thermal weight loss between 50-150 °C is probably attributed to water desorption. As shown in Figure 6, the parent MCM-41 contained 9% of physically adsorbed water, but modified samples contained approximately 12% of adsorbed solvents. Heating of the samples resulted in desorption of solvent molecules from the modification process. The weight loss observed in the region of 150-600 °C (26 wt.%), arose from complete decomposition of the organic modifier, which indicates that the BSA loading on MCM-41 was approximately 26 wt.%. In particular, the weight loss in the range 340 to 600 °C (22 wt.%) resulted from dehydroxylation or removal of BSA from the surface of the sample. TG analysis combined with the FTIR data demonstrated the high stability of the grafted organic layer.

3.1.6 Acidity and elemental analysis

The acidity and elemental analysis were also used to characterize the catalysts. The Brønsted acidity of the two catalysts was determined from Hammett plots obtained using a UV–visible spectrophotometer with 4-nitroaniline as an indicator. Table 2 shows that the Brønsted acidity of BSA/MCM-41 is much higher than MCM-41, indicating that the grafting process increased the acidity. Moreover, the sulfur content was determined by Elemental Analysis using a Fisons Instruments EA 1108 (CHNS-O). From the elemental analysis

results in Table 2, w(S) = 8.33, which is in good agreement with the values obtained by thermogravimetry, further proving that BSA has been successfully grafted onto MCM-41.

Table 2.   The S content and acidity of samples

Entry	Catalyst	S [%]	H_0
1	MCM-41	0	6.86
2	BSA/MCM-41	8.33	0.81

3.2 Catalytic performance study for CL-20 production

3.2.1 Activity of the BSA/MCM-41 catalyst

To compare the catalytic activity of different catalysts, such as MCM-41 and BSA/MCM-41, their catalytic activities were studied in the specified reaction. As can be concluded from Figure 7, the changes in yield and purity of CL-20 *versus* reaction time for different catalysts showed similar trends. At the beginning of the reaction, the yield and purity of CL-20 increased with increasing reaction time during 3 h for the BSA/MCM-41 and 5 h for both the MCM-41 and a non-catalyst. The yield and purity increased slowly and did not increase further even on increasing the reaction time to 7 h. The BSA/MCM-41 catalyst exhibited an outstanding catalytic performance leading to a high yield and purity of CL-20 (yield >90.9% and purity >96.6%) after 3 h, while both MCM-41 and non-catalyst showed low activity. Showing a direct relationship between catalytic activity and the acidity of the active phase, these results indicated that the acidity of the BSA/MCM-41 catalyst played a vital role in the nitration of TAIW to give CL-20. In this study, shorter and longer reaction times could not improve the reaction yield and purity. With longer reaction time, perhaps cage decomposition occurs and with shorter reaction times, the reactions were incompleted. BSA/MCM-41 was the most effective catalyst for this reaction, presumably due to its higher Brønsted acid activity.
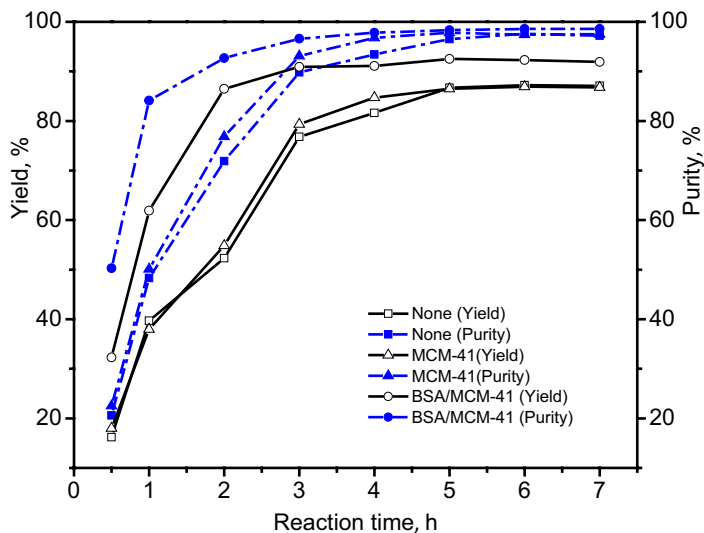
Figure 7. Catalytic activity of different catalysts on the nitration yield and purity of CL-20

3.2.2 Effect of the amount of BSA/ MCM-41 catalyst

The effect of the amount of BSA/MCM-41 on the reaction yield and purity were investigated. In this study, the amount of the prepared BSA/MCM-41 was varied within the range 0.1-0.9 g. As shown in Figure 8, the results indicated that the reaction yield and purity improved with an increase in the amount of catalyst. This could be due to the external surface area with an increasingly accessible amount of acidic sites on the catalyst. By contrast, by using a larger amount of catalyst the yield decreased. This may be due to the greater solid acidic environment as well as a reduction in mobility, and consequently cage decomposition. Furthermore, the optimized amount of the BSA/MCM-41 was found to be 0.5 g in Figure 8.
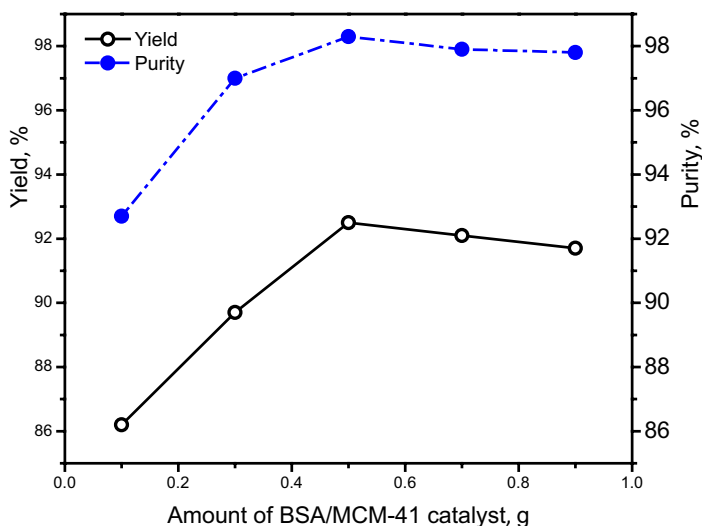
Figure 8.   Optimization of the amount of BSA/MCM-41 catalyst on the nitration yield and purity of CL-20

3.2.3 Reuse of the catalyst

The reusability of the catalyst was studied in five consecutive runs. After each run, the BSA/MCM-41 catalyst was filtered off, washed exhaustively with EtOAc, and then dried. The recycled catalyst was then tested in a futher reaction. As seen in Figure 9, it was found that the reactivity of the recycled BSA/MCM-41 was preserved after five consecutive runs (yield >90.3% and purity >95.5%), which indicated the BSA/MCM-41 catalyst promotes the reaction with remarkable retention of catalytic activity each time. Moreover, examination of the FTIR spectra of BSA/MCM-41 before and after the regeneration, indicated that the structure of BSA/MCM-41 is sufficiently stable during the recycling process. All of these results proved that the interactions between the BSA groups and MCM-41 could decrease the probability of leaching of BSA occurring.
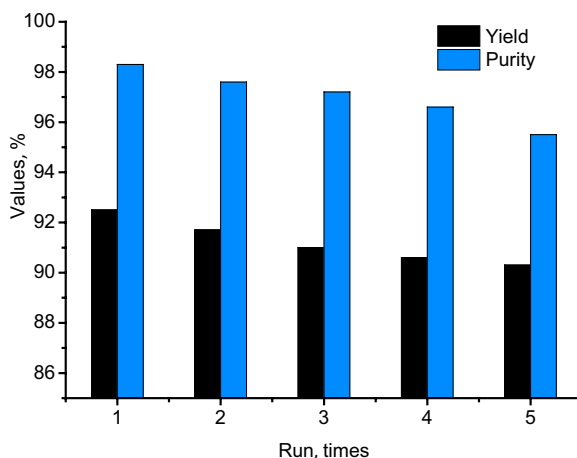
Figure 9.   Recyclability of BSA/MCM-41 catalyst in five consecutive runs

4   Conclusions

In summary, CL-20 had been prepared using successfully grafted BSA/MCM-41, which retains the porous structure of the original MCM-41 silica, as a strong, environmentally benign and effective heterogeneous catalyst. Although the grafted organic layer was slightly damaged, a relatively high BET surface area and high stability were still maintained. Compared with MCM-41 and non-catalysts, the BSA/MCM-41 catalyst has the following advantages:

(i)   It has a higher Brønsted acid activity, resulting from the mass of benzene sulphonic acid groups adsorbed on the surface of the MCM-41 during functionalisation;

(ii)   The BSA/MCM-41, as the solid acid catalyst, has shown the best catalytic activity because it reduces the reaction time by 2 h;

(iii) The catalyst can be reused several times without any remarkable loss of its catalytic potential;

(iv)   The optimized amount of the BSA/MCM-41 was found to be 0.5 g (for 4.5 g TAIW);

(v)   A crude yield of 92.5% with 98.3% purity have been obtained in the nitration reaction under the optimized condition (5 h, 343.15 K, 40 mL 98% HNO_3 electrolyte, 0.5 g BSA/MCM-41 and 4.5 g TAIW).

References

[1] Nielsen, A.T.; Chan, M.L.; Kraeutle, C.K. *Polynitropolyazacaged Explosives, Part 7.* NWC TP 7200[R], China Lake Naval Weapons Center, **1989**.

[2] Nair, U.R.; Asthana, S.N.; Rao, A.S.; Gandhe, B.R. Advances in High Energy Materials. *Def. Sci. J.* **2010**, *60*: 137-151.

[3] Agrawal, J.P. Some New High Energy Materials and Their Formulations for Specialized Applications. *Propellants Explos. Pyrotech.* **2005**, *30*: 316-332.

[4] Nair, U.; Sivabalan, R.; Gore, G.; Geetha, M.; Asthana, S.; Singh, H. Hexanitrohexaazaisowurtzitane (CL-20) and CL-20-Based Formulations. *Combust. Explos. Shock Waves* **2005**, *41*: 121-132.

[5] Latypov, N.V.; Wellmar, U.; Goede, P.; Bellamy, A.J. Synthesis and Scale-Up of 2,4,6,8,10,12-Hexanitro-2,4,6,8,10,12-hexaazaisowurtzitane from 2,6,8,12-Tetraacetyl-4,10-dibenzyl-2,4,6,8,10,12-hexaazaisowurtzitane (HNIW, CL-20). *J. Org. Process Res. Dev.* **2000**, *4*(3): 156-158.

[6] Bayat, Y.; Ahari Mostafavi, M.M.; Hasani, N. [Hmim][HSO$_4$], a Green and Recyclable Acidic Ionic Liquid Medium for the One-Pot Nitration of TADB to HNIW. *Propellants Explos. Pyrotech.* **2014**, *39*: 649-652.

[7] Yan, G.; Yang, M. Recent Advances in the Synthesis of Aromatic Nitro Compounds. *Cheminform.* **2013**, *44*: 2554-2566.

[8] Sheemol, V.; Tyagi, B.; Jasra, R. Nitration of O-xylene over Rare Earth Cations Exchanged Zeolite-b with Nitric Acid and Acetic Anhydride. *J. Mol. Catal. A: Chem.* **2006**, *252*: 194-201.

[9] Bayat, Y.; Hajighasemali, F. [Hmim][HSO$_4$], Synthesis of CL-20 by a Greener Method Using Nitroguanidine/HNO$_3$. *Propellants Explos. Pyrotech.* **2016**, *41*: 20-23.

[10] Hu, X.L.; Wu, Q.J.; Qian, H. Synthesis of CL-20 by Nitrolysis of TAIW with N$_2$O$_5$/HNO$_3$. (in Chinese) *Chin. J. Explos. Propellants (Huozhayao Xuebao)* **2015**, *38*: 35-38.

[11] Kai, W.; Dong, B.; Yang, C.F.; Qian, H. Acidic Ionic Liquids and Green and Recyclable Catalysts in the Clean Nitration of TAIW to CL-20 Using HNO$_3$ Electrolyte. *Can. J. Chem.* **2017**, *95*: 190-193.

[12] Shi, L.; Kai, W.; Yang, C.-F.; Qian, H.; Liu, D.-B.; Pan, R.-M. Synthesis, Characterization of Nafion-functionalized MCM-41 and Its Catalytic Application in Preparation of CL-20 *via* HNO$_3$ Electrolyte Involved Nitration of TAIW. *J. Saudi Chem. Soc.* **2018**, *22*: 588-593.

[13] Bu, L.; Dong, B.; Qian, H.; Zhen, J. Economic Preparation of CL-20 by Nitrolysis of TAIW Using Surfactants as Catalyst. (in Chinese) *Explosive Materials* **2016**, *45*: 25-28.

[14] Dong, B.; Qian, H.; Ren, L.P. A Nitrolysis Method to Synthesize CL-20 with High Yield and Low Pollution. (in Chinese) *Chin. J. Energ. Mater.* (*Hanneng Cailiao*) **2016**, *24*: 571-575.

[15] Mizuno, N.; Misono, M. Heteropolyacid Catalysts. *Curr. Opin. Solid St. M. Sci.*

      1997, (2): 84-89.
[16] Fotouhi-Far, F.; Bashiri, H.; Hamadanian, M. Study of Deactivation of Pd(OH)$_2$/C
      Catalyst in Reductive Debenzylation of Hexabenzylhexaazaisowurtzitane.
      Propellants Explos. Pyrotech. **2017**, *42*(2): 213-219.
[17] Fotouhi-Far, F.; Bashiri, H.; Hamadanian, M.; Keshavarz, M.H. Increment
      of Activity of Pd(OH)$_2$/C Catalyst in Order to Improve the Yield of High
      Performance 2,4,6,8,10,12-hexanitrohexaazaisowurtzitane (HNIW). *Inorg. Nano-
      Met. Chem.* **2017**, *47*(11): 1489-1494.
[18] Harrar, J.E.; Pearson, R.K. Electrosynthesis of N$_2$O$_5$ by Controlled-Potential
      Oxidation of N$_2$O$_4$ in Anhydrous HNO$_3$. *J. Electrochem. Soc.* **1983**, *130*: 108-112.
[19] Harrar, J.E.; Quong, R.; Rigdon, L.P.; McGuire, R.R. Scale-Up Studies
      of the Electrosynthesis of Dinitrogen Pentoxide in Nitric Acid. *J. Electrochem.
      Soc.* **1997**, *144*(6): 2032-204.
[20] Marshall, R.J.; Shiffin, D.J.; Walsh, W.C.; Bagg, G.E.G. *The* Electrochemical
      Generation of *N$_2$O$_5$*. Patent EP 0295878B1, **1991**.
[21] Chapman, R.D.; Smith, G.D. Separation of Dinitrogen Pentoxide from Its Solutions
      in Nitric Acid. In: *Nitration* (Albright, L.F.; Carr, R.V.C.; Schmitt, R.J., Eds), American
      Chemical Society: Washington, **1996**, Chapter 9, p. 78; ISBN: 9780841233935.
[22] Estifaee, P.; Haghighi, M.; Babaluo, A.A.; Rahemi, N.; Fallah Jafari, M.
      The Beneficial Use of Non-thermal Plasma in Synthesis of Ni/Al$_2$O$_3$-MgO
      Nanocatalyst Used in Hydrogen Production from Reforming of CH$_4$/CO$_2$
      Greenhouse Gases. *J. Power Sources* **2014**, *257*: 364-373.
[23] Abbasi, Z.; Haghighi, M.; Fatehifar, E.; Saedy, S. Synthesis and Physicochemical
      Characterization of Nanostructured Pt/CeO$_2$ Catalyst Used for Total Oxidation
      of Toluene. *Int. J. Chem. Reactor Eng.* **2011**, (9): 1-19.
[24] Khoshbin, R.; Haghighi, M. Urea-nitrate Combustion Synthesis and Physicochemical
      Characterization of CuO-ZnO-Al$_2$O$_3$ Nanoparticles over HZSM-5. *Chin. J. Inorg.
      Chem.* **2012**, *28*(9): 1967-1978.
[25] Jamalzadeh, Z.; Haghighi, M.; Asgari, N. Synthesis, Physicochemical
      Characterizations and Catalytic Performance of Pd/Carbon-Zeolite and Pd/Carbon-
      CeO$_2$ Nanocatalysts Used for Total Oxidation of Xylene at Low Temperatures.
      Front. Environ. Sci. Eng. **2013**, (7): 365-381.
[26] Sajjadi, S.M.; Haghighi, M.; Eslami, A.A.; Rahmani, F. Hydrogen Production
      via CO$_2$-Reforming of Methane Over Cu and Co Doped Ni/Al$_2$O$_3$ Nanocatalyst:
      Impregnation *versus* Sol-gel Method and Effect of Process Conditions and Promoter.
      J. Sol-Gel. Sci. Technol. **2013**, *67*: 601-617.
[27] Vafaeian, Y.; Haghighi, M.; Aghamohammadi, S. Ultrasound Assisted Dispersion
      of Different Amount of Ni Over ZSM-5 Used as Nanostructured Catalyst
      for Hydrogen Production *via* CO$_2$ Reforming of Methane. *Energy Convers. Manage.*
      2013, *76*: 1093-1103.
[28] Buzzoni, R.; Bordiga, S.; Ricchiardi, G.; Spoto, G.; Zecchina, A. Interaction of H$_2$O,
      CH$_3$OH, (CH$_3$)$_2$O, CH$_3$CN, and Pyridine with the Superacid Perfluorosulfonic
      Membrane Nafion: An IR and Raman Study. *J. Phys. Chem.* **1995**, *99*: 307-311.

[29] Zecchina, A.; Geobaldo, F.; Spoto, G.; Bordiga, S.; Ricchiardi, G.; Buzzoni, R.; Petrini, G. FTIR Investigation of the Formation of Neutral and Ionic Hydrogen-Bonded Complexes by Interaction of H-ZSM-5 and H-Mordenite with CH_3CN and H_2O: Comparison with the H-NAFION Superacidic System. *J. Phys. Chem.* **1996**, *100*: 16584-16599.

[30] Mercedes, A.; Avelino, C.; Debasish, D.; Vicente, F.; Hermenegildo, G. "Nafion"-functionalized Mesoporous MCM-41 Silica Shows High Activity and Selectivity for Carboxylic Acid Esterification and Friedel-Crafts Acylation Reactions. *J. Catal.* **2005**, *231*: 48-55.

[31] Sing, K.S.W.; Everrett, D.H.; Haul, R.A.W.; Moscow, L.; Pierotti, R.A.; Rouquerol, J.; Siemieniewska, T. Reporting Physisorption Data for Gas/Solid Systems with Special Reference to the Determination of Surface Area and Porosity. *Pure Appl. Chem.* **1985**, *57*: 603-619.

[32] Zhang, C.; Yu, M.J.; Pan, X.Y. Regioselective Mononitration of Chlorobenzene Using Caprolactam-based Brønsted Acidic Ionic Liquids. *J. Mol. Catal. A: Chem.* **2014**, *383*: 101-105.